Title

Genetic and transcriptomic dissection of nitrate-independent function of Arabidopsis NRT1.1/NPF6.3/CHL1 under high ammonium condition

Authors and addresses

Takushi Hachiya[a,b,†], Nobue Makita[b], Liên Bach[c], Alain Gojon[c], Tsuyoshi Nakagawa[a], and Hitoshi Sakakibara[b,d]

[a]Department of Molecular and Functional Genomics, Interdisciplinary Center for Science Research, Shimane University, Matsue 690-8504, Japan

[b]RIKEN Center for Sustainable Resource Science, Tsurumi, Yokohama 230-0045, Japan

[c]Institut des Sciences des Plantes de Montpellier (IPSiM), Université de Montpellier, Centre National de la Recherche Scientifique (CNRS), Institut National de Recherche pour l'Agriculture, l'Alimentation, et l'Environnement (INRAE), Institut Agro, Montpellier, France

[d]Graduate School of Bioagricultural Sciences, Nagoya University, Nagoya 464-8601, Japan

Corresponding Author

Takushi Hachiya

Department of Molecular and Functional Genomics, Interdisciplinary Center for Science Research, Shimane University, Matsue 690-8504, Japan

Email: takushi.hachiya@life.shimane-u.ac.jp,

Tel: +81-852-32-6288, FAX: +81-852-32-6109

Abstract

The Arabidopsis nitrate transceptor NRT1.1/NPF6.3/CHL1 regulates physiological responses to nitrate. Several studies have reported that Arabidopsis plants lacking NRT1.1 show enhanced shoot growth under toxic levels of ammonium without nitrate, suggesting a nitrate-independent function for NRT1.1. To further investigate this nitrate-independent function and its impact on ammonium tolerance, we conducted genetic analysis, tissue-specific expression analysis, and transcriptome analysis using various NRT1.1-related lines. Transgenic plants expressing either nonphosphomimic or phosphomimic mutants of NRT1.1 exhibited similar ammonium tolerance to the wild-type. The *chl1-9* mutant, in which NRT1.1 with the P492L substitution is localized intracellularly rather than at the plasma membrane and fails to transport nitrate, showed significantly improved ammonium tolerance. Confocal imaging revealed that the NRT1.1-GFP signal was detected in the plasma membrane of various tissues, including cotyledon pavement cells, hypocotyl epidermal cells, mesophyll cells, root cap cells, and epidermal cells near root tips. In early seedlings, the absence of functional NRT1.1 altered the expression of genes associated with aliphatic glucosinolate biosynthesis, ethylene signaling, and low pH stress. Genes predicted to encode products localized to the extracellular space were enriched among those differentially expressed due to *NRT1.1* deficiency. Our data suggest that in the absence of nitrate, plasma membrane-targeted NRT1.1 reduces ammonium tolerance irrespective of its phosphorylation state with alterations of gene expression associated with stress and senescence.

Key words: ammonium toxicity, CHL1, NPF6.3, NRT1.1

67 **1. Introduction**

68 Most land plants primarily rely on soil nitrate as their main nitrogen (N) source. Nitrate
69 serves not just as a substrate for N assimilation but also as a vital signaling molecule,
70 regulating genes related to nitrogen acquisition and root system development (Wang et
71 al. 2004; Okamoto et al. 2019). These nitrate responses require molecular components
72 to perceive nitrate and to drive nitrate-dependent signaling. The Arabidopsis nitrate
73 transporter NRT1.1/NPF6.3/CHL1 plays a crucial role as a nitrate sensor, orchestrating
74 various plant responses to nitrate supply (Remans et al. 2006; Ho et al. 2009; Bouguyon
75 et al. 2015). Downstream of NRT1.1, calcium ions serve as secondary messengers,
76 stimulating the expression of nitrate-responsive genes, including the major high-affinity
77 nitrate transport gene *NRT2.1* (Riveras et al. 2015). Recent findings indicate that the
78 subgroup III protein kinase CPK perceives calcium signals and phosphorylates the
79 transcription factor NLP7 (Liu et al. 2017), which directly binds intracellular nitrate,
80 regulating nitrate-dependent gene expression (Liu et al. 2022). Furthermore, NRT1.1
81 enhances the expression of the transcription factor *ANR1* and the *AFB3* auxin receptor
82 gene in roots, promoting lateral root development and elongation in response to nitrate
83 supply (Remans et al. 2006; Vidal et al. 2010). The magnitude of these
84 NRT1.1-dependent responses is finely tuned by the phosphorylation status of NRT1.1 at
85 the T101 residue (Ho et al. 2009; Bouguyon et al. 2015).

86 In addition to its nitrate-dependent functions, NRT1.1 exhibits significant roles in
87 the absence of nitrate. It aids the basipetal transport of auxin out of the lateral root
88 primordia when nitrate is absent (Krouk et al. 2010). Exogenous nitrate inhibits auxin

89 transport, leading to auxin accumulation in primordia and the stimulation of lateral root
90 emergence in nitrate-rich patches (Mounier et al. 2014). Walch-Liu and Forde (2008)
91 observed that exogenous glutamate inhibits primary root elongation at the root tip, a
92 process antagonized by nitrate presence, depending on phosphorylated NRT1.1.
93 Intriguingly, overexpression of nonphosphomimetic NRT1.1 (T101A) heightens
94 glutamate sensitivity in primary roots even without nitrate. Furthermore, studies
95 including ours have demonstrated that the absence of functional NRT1.1 significantly
96 alleviates growth suppression and chlorosis under toxic ammonium levels as the sole N
97 source (Hachiya et al. 2011; Jian et al. 2018; Liu et al. 2020). NRT1.1 promotes
98 ammonium accumulation, altering ammonium metabolism and subsequently
99 upregulating ethylene signaling, resulting in ammonium toxicity (Jian et al. 2018).
100 Moreover, under high ammonium and NaCl concentrations without nitrate, NRT1.1
101 transports chloride, leading to chloride accumulation, especially in roots (Liu et al.
102 2020). This chloride accumulation contributes to ammonium toxicity under high salt
103 conditions.

104 The aforementioned observations clearly indicate a nitrate-independent function for
105 NRT1.1, although the precise mechanism remains elusive. This study aimed to
106 comprehensively uncover the primary nitrate-independent function of NRT1.1 in
107 ammonium tolerance. Employing various NRT1.1-related lines, we conducted genetic
108 analyses, tissue-specific expression studies using quantitative PCR (qPCR) and confocal
109 microscopy, and transcriptome analyses. Our findings reveal that (i) plasma
110 membrane-targeted NRT1.1 diminishes ammonium tolerance regardless of its

111 phosphorylation state, (ii) NRT1.1 is expressed across most seedling tissues, and (iii)
112 NRT1.1 primarily modulates the expression of genes associated with aliphatic
113 glucosinolate (GSL) biosynthesis, ethylene signaling, and low pH stress.
114

115 **2. Materials and Methods**

116 ***2.1. Plant materials and growth conditions***

117 In this study, Arabidopsis plants were used. The T-DNA insertion mutants *nrt1.1*
118 (Hachiya et al. 2011), *cipk23-4* (Ho et al. 2009), and the gamma ray-mutagenized
119 mutant c*hl1-5* (Tsay et al. 1993a) in the Col background were obtained from the
120 European Arabidopsis Stock Center (NASC). The gamma-ray-mutagenized mutant
121 *chl1-6* in the L*er* background (Tsay et al. 1993b) was sourced from the Arabidopsis
122 Biological Resource Center. The transposon tag line *pst16286* in the Nossen
123 background (Ito et al. 2002; Kuromori et al. 2004) was purchased from the RIKEN
124 Bioresource Center (BRC). The lines harboring the estradiol-inducible
125 *NRT1.1-mCherry* and the *pNRT1.1:NRT1.1-GFPloop* in the *chl1-5* background were
126 used in previous studies (Bouguyon et al. 2015; Bouguyon et al. 2016). The *chl1-9* in
127 the Col background and the *T101D* and *T101A* lines in the *chl1-5* background (Ho et al.
128 2009) were provided by Dr. Yi-Fang Tsay (Academia Sinica).

129 The seeds underwent surface sterilization and were placed in plastic Petri dishes
130 (diameter: 90 mm; depth: 20 mm; Iwaki, Tokyo, Japan) with approximately 30 mL of
131 N-modified Murashige and Skoog medium. The medium included 4.7 mM MES-KOH
132 (pH 5.7), 2% (w/v) sucrose, and 0.25% (w/v) gellan gum (Wako, Osaka, Japan). Two

133 different N and K sources were used: 10 mM KNO_3 (10 mM NO_3^- condition) or 5 mM
134 $(NH_4)_2SO_4$ with 10 mM KCl (10 mM NH_4^+ condition). After being kept in the dark at
135 4 °C for 3 d, the plants were grown horizontally under a photosynthetic photon flux
136 density of 100–130 μmol m^{-2} s^{-1} (16 h light/8 h dark cycle) at 23 °C. For transfer
137 experiments, surface-sterilized seeds were sown in larger plastic Petri dishes (length:
138 140 mm; width: 100 mm; depth: 20 mm; Eiken Chemical Co. Ltd., Taito-ku, Tokyo,
139 Japan) containing 50 mL of half-strength modified Murashige and Skoog medium with
140 2.5 mM ammonium as the sole N source at pH 6.7 (Okamoto et al. 2019). After 3 days
141 in the dark at 4 °C, the plants were grown vertically for 5 d under a photosynthetic
142 photon flux density of 100–130 μmol m^{-2} s^{-1} (16 h light/8 h dark cycle) at 23 °C. The
143 plants were then transferred to different N conditions for subsequent experiments.
144 Further details regarding plantlet cultivation are provided in the Results section and
145 figure legends.

146 ***2.2. Extraction of RNA***

147 The whole seedlings, shoots, and roots were harvested and promptly frozen in liquid N_2,
148 then stored at −80 °C until needed. The frozen samples were ground using TissueLyser
149 II (QIAGEN) with zirconia beads (5 mm diameter). Total RNA was extracted using the
150 RNeasy Plant Mini Kit (Qiagen) and treated with on-column DNase digestion following
151 the manufacturer's instructions.

152 ***2.3. RT-qPCR***

153 Reverse transcription (RT) was conducted using ReverTra Ace qPCR RT Master Mix
154 with gDNA Remover (Toyobo Co. Ltd., Tokyo, Japan) following the manufacturer's

155 guidelines. The resulting cDNA was diluted tenfold with distilled water for quantitative
156 PCR (qPCR). Transcript levels were assessed using a StepOnePlus Real-Time PCR
157 System (Thermo Fisher Scientific, Waltham, MA, USA). In the presence of 10-μL
158 KAPA SYBR FAST qPCR Kit (Nippon Genetics Co. Ltd., Tokyo, Japan), 0.4 μL
159 specific primers (0.2 μM final concentration), and 7.2 μL sterile water, 2 μL of obtained
160 cDNA was amplified. *ACTIN3* (Hachiya et al. 2021) served as internal standards.
161 Standard curves were generated using plasmid DNA containing target cDNAs or total
162 cDNAs. Refer to Supplementary Table 1 for primer sequences.

163 ***2.4. Microarray analysis***

164 Microarray analysis was conducted using 3-day-old (72 h) and 5-day-old (120 h) whole
165 seedlings of Col, *chl1-5*, and *nrt1.1* following the protocol outlined in Hachiya et al.
166 (2021). RNA quality was evaluated using an Agilent 2100 bioanalyzer (Agilent
167 Technologies). RNA amplification, labeling, hybridization, and scanning were
168 performed using the 3′ IVT Express Kit (Affymetrix) and GeneChip Arabidopsis
169 Genome ATH1 Array (Affymetrix) as per the manufacturer's instructions. Data from
170 the microarray chips were normalized using the Microarray Suite 5.0 (MAS5) method
171 (Affymetrix). Transcripts labeled as "absent" or "marginal" were excluded from
172 subsequent quantitative analysis. The raw microarray data used in this study are
173 accessible in the ArrayExpress database at EMBL-EBI under accession number
174 E-MTAB-13395.

175 ***2.5. Observation of cotyledon***

176 Bright-field imaging of Arabidopsis early seedling cotyledons was conducted using an
177 all-in-one fluorescence microscope (BZ-X710, KEYENCE, Japan) equipped with a
178 Nikon 40× objective (CFI Plan Apo λ 40×/0.95). To create a high-resolution and
179 wide-area continuous image of the cotyledon, individual images were seamlessly
180 merged using the image joint function of the BZ analyzer software (KEYENCE).

181 ***2.6. Observation of fluorescent signal***

182 Confocal imaging of NRT1.1-GFPloop and propidium iodide (PI) was performed using
183 a Leica SP5 Confocal Microscope (Leica Microsystems). Roots were stained with a 10
184 μg mL^{-1} PI solution to outline cell shapes. Mesophyll protoplasts were prepared from
185 cotyledons of 12-day-old plants (Plants grown under 10 mM nitrate for 9 days were
186 transferred to 10 mM ammonium and grown for 3 days.) following the method of Endo
187 et al. (2016). NRT1.1-GFPLoop and PI were excited with 488 nm and 543 nm lasers,
188 and emissions were detected from 500 to 530 nm and 590 to 660 nm, respectively,
189 using a Leica 25× objective (HCX IRAPO L 25×/0.95 WATER).

190 ***2.7. Statistical analysis***

191 The unpaired two-tailed Welch's *t*-test and the Tukey–Kramer multiple comparison test
192 were conducted using R software v.2.15.3. Additionally, the two-tailed ratio paired
193 t-test was performed using GraphPad Prism software v.9.3.1, assuming a Gaussian
194 distribution.

195

196 **3. Results**

197 ***3.1. NRT1.1 targeted to the plasma membrane reduces ammonium tolerance almost***
198 ***regardless of its phosphorylation status***

199 In our previous study, *NRT1.1*-deficient mutants in the Col background exhibited
200 enhanced shoot growth under 10 mM ammonium conditions (Hachiya et al. 2011). In
201 this study, we consistently observed larger shoot fresh weights (FWs) in
202 *NRT1.1*-deficient mutants from three Arabidopsis accessions (Col; *chl1-5*, *nrt1.1*, *Ler*;
203 *chl1-6*, and Nossen; *pst16286*) compared to wild-type plants under 10 mM ammonium.
204 Conversely, under 10 mM nitrate conditions, the FWs were lower in these mutants
205 (Figure 1a, b). Intriguingly, the induction of NRT1.1-mCherry in the *chl1-5* background,
206 controlled by β-estradiol (Bouguyon et al. 2015), significantly reduced shoot FW under
207 ammonium, whereas β-estradiol-treated Col plants did not show a change in FW
208 (Figure 1c). Under nitrate, shoot growth was restored by the induction of
209 NRT1.1-mCherry, confirming its functionality (Figure 1d). These findings underscore
210 the significant role of Arabidopsis NRT1.1 in ammonium tolerance.

211 NRT1.1 exhibits diverse molecular functions, including nitrate uptake, nitrate
212 sensing/signaling, and auxin transport (Ho et al. 2009; Krouk et al. 2010; Bouguyon et
213 al. 2015; Zhang et al. 2019). Modifications at specific residues in the protein alter these
214 functions. In the *chl1-9* mutant with the P492L substitution, NRT1.1 primarily localizes
215 intracellularly rather than at the plasma membrane (Bouguyon et al. 2015). Surprisingly,
216 whilst P492L lacks the ability to transport nitrate and auxin, it can still drives some of
217 the nitrate-dependent signaling, including short-term induction of *NRT2.1* by nitrate (Ho
218 et al. 2009; Bouguyon et al. 2015). This suggests that NRT1.1 functions as a nitrate

219 sensor, independent of its uptake activity. The phosphorylation status of NRT1.1 at the
220 T101 residue alters its affinity for nitrate; Non-phosphorylated NRT1.1 forms a
221 homodimer with the NRT1.1 located in close proximity to the dimer interface, allowing
222 low-affinity nitrate uptake, whereas phosphorylated NRT1.1 decouples the dimer
223 configuration to act as a high-affinity nitrate transporter (Sun and Zheng 2015).
224 Moreover, the phosphorylated form transports auxin better than the non-phosphorylated
225 form in the absence of nitrate (Bouguyon et al. 2015). To reveal how P492L substitution
226 and phosphorylation status of NRT1.1 affects ammonium tolerance, we analyzed
227 growth of *chl1-9* and transgenic plants expressing nonphosphomimic (T101A) or
228 phosphomimic (T101D) mutants of NRT1.1.

229 When grown on 10 mM ammonium, the *chl1-9* mutant exhibited markedly
230 improved ammonium tolerance compared to the wild-type, displaying larger FWs and
231 higher chlorophyll concentrations (Figure 1e–g). Except for slightly enhanced shoot
232 growth in T101A compared to Col, both T101 mutants displayed ammonium toxicity
233 similar to Col. Moreover, *cipk23-4*, lacking CIPK23 that phosphorylates NRT1.1 at the
234 T101 residue (Ho et al. 2009), did not exhibit enhanced shoot growth under ammonium
235 or nitrate conditions (Figure 1h, i). These results imply that NRT1.1-induced
236 ammonium toxicity is nearly independent of its phosphorylation at the T101 residue but
237 requires correct plasma membrane targeting dependent on the P492 residue. Given that
238 the phosphorylating status alters auxin transport in the absence of nitrate (Bouguyon et
239 al. 2015), changes in auxin distribution and action may have little effect on ammonium
240 toxicity.

241 To determine the developmental stages at which NRT1.1 affects ammonium
242 tolerance, we monitored the growth progression of Col and *chl1-5* plants under 10 mM
243 ammonium. In 3-day-old seedlings, there were no significant difference in FW, and
244 their appearances were similar (Figure 1j, l). By day 5, *chl1-5* seedlings exhibited larger
245 shoot and root FWs, and their cotyledons were more expanded and greener compared to
246 Col (Figure 1k, l, and S1a). Additionally, at this stage, *chl1-5* and *nrt1.1* seedlings had
247 significantly higher chlorophyll concentrations than Col (Figure S1b). As plants aged
248 between 8 and 11-days, the impact of *NRT1.1* deficiency on shoot growth intensified
249 compared to root growth (Figure 1k). These findings highlight that NRT1.1's influence
250 on ammonium tolerance initiates at the early stages of seedling growth.

251 ***3.2. A significant expression of NRT1.1 is detectable both in shoots and roots of***
252 ***ammonium-grown seedlings***

253 To decipher how NRT1.1 impacts ammonium tolerance, we examined *NRT1.1*
254 expression patterns in Col plants grown under 10 mM ammonium or 10 mM nitrate. In
255 3-day-old Col seedlings, *NRT1.1* expression showed little disparity between ammonium
256 and nitrate conditions (Figure 2a). However, in 5-, 8-, and 11-day-old plants, shoot
257 expression of *NRT1.1* remained consistently higher under 10 mM ammonium compared
258 to 10 mM nitrate, whereas in the roots, this trend reversed (Figure 2b). Consequently,
259 the disparity in *NRT1.1* transcript levels between shoot and root was smaller under
260 ammonium than nitrate. Furthermore, to investigate NRT1.1 protein expression under
261 ammonium conditions, we utilized the *pNRT1.1:NRT1.1-GFPloop* line for confocal
262 observation (Bouguyon et al. 2016). Clear GFP signals were localized in the plasma

263 membrane of various cells, including pavement cells of cotyledons (Figure 2c, i),
264 epidermal cells of hypocotyl (Figure 2d), mesophyll protoplasts (Figure 2e), root cap
265 cells, and epidermal cells near primary root tips (Figure 2f, g). Intriguingly, dotted GFP
266 signals were frequently detected in intracellular regions of pavement cells and root tips
267 (Figure 2h, j). These expression analyses indicate that NRT1.1 might function in diverse
268 cells and tissues under high ammonium conditions.

269 ***3.3. Overview of genome-wide transcriptional responses caused by NRT1.1 deficiency***

270 To unravel the primary mechanisms by which NRT1.1 controls genome-wide gene
271 expression under ammonium conditions, we conducted independent microarray
272 experiments using 3-day-old (72 h) and 5-day-old (120 h) whole seedlings of Col,
273 *chl1-5*, and *nrt1.1*. In 3- and 5-day-old seedlings, we identified 20 and 176 transcripts,
274 respectively, in which expression was at least two-fold higher in both *NRT1.1*-deficient
275 mutants compared to Col (Table S2). Conversely, 13 and 80 transcripts in the mutants
276 exhibited levels less than or equal to half of those in Col (Table S2). To capture more
277 NRT1.1-regulated genes in the 3-day-old seedlings, we re-explored differentially
278 expressed genes (DEG) at a 1.5-fold threshold. This analysis identified 120 upregulated
279 genes and 71 downregulated genes in the mutants relative to Col (Table S3). RT-qPCR
280 analysis of 12 DEGs confirmed that the results were consistent with those of the
281 microarray (Figure S2 and Tables S2, 3). For subsequent analyses, we concentrated on
282 DEGs at a 1.5-fold threshold for 3-day-old seedlings and a 2-fold threshold for
283 5-day-old seedlings. A Venn diagram revealed that only 26 DEGs were common to both
284 3-day-old and 5-day-old seedlings (Figure 3a and Table S4). Enrichment analysis

285 conducted using Metascape (Zhou et al. 2019) identified a significant enrichment of the
286 term "response to extracellular stimulus" (Figure S3a). Additionally, the SUBA
287 localization predictor (Hooper et al. 2017) indicated that the translational products
288 corresponding to 9 out of the 26 DEGs were likely localized in the extracellular space
289 (Figure S3b). These findings suggest that, under ammonium conditions, NRT1.1 could
290 influence extracellular events.

291 In 3-day-old seedlings, the absence of NRT1.1 led to significant gene expression
292 changes without altering seedling growth (Figure 1e, 3a). Thus, we focused on the
293 transcriptome profile of 3-day-old seedlings to uncover the primary functions of
294 NRT1.1 under ammonium conditions. Gene cloud analysis (Krouk et al. 2015) revealed
295 a 168-fold enrichment in "methionine-derived" and a 120-fold enrichment in
296 "4-reductase" genes in the upregulated genes of 3-day-old *NRT1.1*-deficient mutants
297 (Figure 3b). "Methionine-derived" genes included *At3g19710* (*BCAT4*), *At4g12030*
298 (*BAT5*), and *At5g23010* (*MAM1*), essential for aliphatic glucosinolate biosynthesis. The
299 "4-reductase" genes included *At2g47460* (*MYB12*), *At4g09820* (*bHLH042*), and
300 *At5g42800* (*DFR*), contributing to flavonoid biosynthesis. Metascape analysis also
301 overrepresented terms like "glucosinolate biosynthesis from methionine" and
302 "flavonoid metabolic process" for upregulated genes in the mutants (Figure 3c).
303 Downregulated genes in the 3-day-old mutants enriched terms like "interpro-ipr008263
304 (glycoside hydrolase, family 16, active site)" from genes encoding cell wall-modifying
305 enzymes like xyloglucan endotransglucosylase/hydrolase (*At4g25810* (*XTH23*),
306 *At4g14130* (*XTH15*), and *At5g57560* (*XTH22*)) (Figure 3b). Intriguingly, DEGs in the

307 3-day-old mutants often overrepresented terms related to the extracellular space, such as
308 "plant-type cell wall loosening," "secretory vesicle," "apoplast," "xyloglucan metabolic
309 process," "plant-type cell wall," and "xyloglucan:xyloglucosyl transferase activity"
310 (Figure 3c, d).

311 In 5-day-old seedlings, terms related to photosynthesis were predominant among
312 upregulated genes in response to *NRT1.1* deficiency (Figure S4a, b). This aligns with
313 the observed greener and more expanded cotyledons and higher chlorophyll
314 concentrations in *NRT1.1*-deficient seedlings compared to Col (Figure 1m and S1a, b).
315 Conversely, downregulated genes were associated with terms related to abiotic and
316 biotic stresses (Figure S4c). MapMan analysis clearly illustrated the upregulation of
317 genes encoding components for light reactions, chlorophyll biosynthesis, and the
318 Calvin–Benson cycle in 5-day-old *NRT1.1*-deficient mutants (Figure S5b). These
319 findings indicate an enhancement of photoautotrophic growth with reduced stress
320 response in the 5-day-old mutants.

321 ***3.4. Effects of NRT1.1 deficiency on expression of genes for glucosinolate***
322 ***biosynthesis and genes responsive to ACC, NaCl, H_2O_2, IAA, and low pH under***
323 ***ammonium condition***

324 Initially, we concentrated on the genes involved in the biosynthesis of aliphatic GSL
325 and indole GSL, based on the gene list from Harun et al. (2020). This focus was due to
326 the enrichment of terms such as "glucosinolate biosynthesis from methionine,"
327 "methionine-derived," and "glucosinolate biosynthesis" among the upregulated genes in
328 3- and 5-day-old *NRT1.1*-deficient mutants (Figures 3b, c, and S5b). The deficiency of

329 *NRT1.1* significantly upregulated the aliphatic GSL biosynthesis genes and their
330 positive regulator genes, *AT5G61420* (*MYB28*) and *AT5G07690* (*MYB29*), while it had
331 little effect on the expression of indole GSL biosynthesis genes (Figure 4a and Tables
332 S2, 3, and 5).

333 Our enrichment analysis revealed that the GO term "cellular response to ethylene
334 stimulus" was overrepresented among the downregulated genes in 3-day-old
335 *NRT1.1*-deficient mutants (Figure 3d). This aligns with a previous study that reported a
336 down-regulation of genes involved in ethylene biosynthesis and senescence under toxic
337 ammonium conditions in *NRT1.1*-deficient mutants (Jian et al. 2018). Consequently, we
338 examined the genes responsive to the application of 1-aminocyclopropane-1-carboxylic
339 acid (ACC), a precursor of ethylene whose biosynthesis is a rate-limiting step for
340 ethylene production, based on the gene list from Goda et al. (2008) (Figure 4b and
341 Table S6). The ACC-induced genes were significantly downregulated in both 3- and
342 5-day-old *NRT1.1*-deficient mutants grown under 10 mM ammonium, whereas the
343 ACC-repressed genes did not show a significant response.

344 The GO term "response to salt stress" was found to be overrepresented in the
345 downregulated genes of 3- and 5-day-old *NRT1.1*-deficient mutants (Figures 3d and
346 S4c). A recent study found that in the presence of a 25 mM chloride ion with
347 ammonium as the sole N source, NRT1.1 supports excessive chloride absorption,
348 resulting in severe root growth inhibition (Liu et al. 2020). *NRT1.1* deficiency may
349 affect the expression of NaCl-responsive genes because our ammonium solution
350 contains 16 mM chloride ions. The NaCl-induced genes listed from Shen et al. (2014)

351 were significantly downregulated in the 5-day-old *NRT1.1*-deficient mutants, but not in
352 the 3-day-old mutants (Figures 4c and Table S7). The expression of NaCl-repressed
353 genes differed little between Col and *NRT1.1*-deficient mutants.

354 It has been reported that ammonium nutrition disrupts redox homeostasis, leading
355 to the apoplastic accumulation of reactive oxygen species and oxidative stress
356 (Podgórska et al. 2015). In line with this, our enrichment analysis revealed the presence
357 of the GO terms "response to oxidative stress" and "antioxidant activity" among the
358 downregulated genes in both 3-day-old and 5-day-old *NRT1.1*-deficient mutants (Figure
359 3d and S4c). Genes that are upregulated in response to H_2O_2 application, as documented
360 by Hieno et al. (2019), were downregulated in the 5-day-old *NRT1.1*-deficient mutants,
361 but not in the 3-day-old mutants (Figure 4d and Table S8). No significant alterations in
362 the expression of genes downregulated by H_2O_2 were observed between Col and the
363 *NRT1.1*-deficient mutants.

364 Regarding auxin responses, although NRT1.1 facilitates auxin influx into the cell
365 in the absence of nitrate (Krouk et al. 2010), its deficiency did not significantly alter the
366 expression of typical genes responsive to indole-3-acetic acid (IAA) application (Goda
367 et al. 2008) (Figure 4e and Table S9).

368 Interestingly, previous studies have shown that 43% of ammonium-inducible genes
369 correspond to low pH (4.5)-inducible genes in Arabidopsis plants (Lager et al. 2010;
370 Patterson et al. 2010). We have previously observed that the enhanced ammonium
371 tolerance of *NRT1.1*-deficient mutants at pH 5.7 was mimicked in Col plants grown at
372 pH 6.7 (Hachiya et al. 2011). These findings suggest that *NRT1.1*-deficient mutants may

373 exhibit enhanced tolerance to ammonium-derived acidic stress. Consequently, we
374 examined the microarray data with a focus on low pH stress-responsive genes listed in
375 Lager et al. (2010). Remarkably, the low pH stress-inducible genes were significantly
376 downregulated both in the 3- and 5-day-old *NRT1.1*-deficient mutants relative to Col,
377 whereas the low pH stress-repressive genes were generally upregulated in the mutants
378 (Figure 4f and Table S10).

379 Collectively, we conclude that NRT1.1 primarily alters the expression of genes
380 associated with aliphatic glucosinolate biosynthesis, ethylene signaling, and low pH
381 stress.

382

383 **4. Discussion**

384 The Arabidopsis nitrate transceptor NRT1.1 and its orthologs are required for plant
385 adaptation to nitrate-rich conditions (Wang et al. 2020). NRT1.1, on the other hand, has
386 been shown to reduce ammonium tolerance in the absence of nitrate (Hachiya et al.
387 2011; Jian et al. 2018). Thus, NRT1.1 and its orthologs are likely to determine adaption
388 features for the two major N sources, nitrate and ammonium.

389 Excessive ammonium assimilation by plastidic glutamine synthetase produces
390 proton accumulation and acidic stress in Arabidopsis shoots when exposed to high
391 amounts of ammonium (Hachiya et al. 2021). Proton excretion from plants to external
392 media is common in plant cultivation with high ammonium feeding (Britto and
393 Kronzucker 2002). Moreover, in Arabidopsis plants, ammonium-inducible genes and
394 low pH (4.5)-inducible genes overlap at a significant rate (Lager et al. 2010, Patterson et

395 al. 2010). These findings imply that acidic stress is a major source of ammonium
396 toxicity. Our transcriptome analysis revealed that *NRT1.1* deficiency dampens low pH
397 responses (Figure 4f). We observed that increasing the pH of the medium from 5.7 to
398 6.7 by adding alkaline NH_3 solution promoted shoot development of Col more intensely
399 than that of *chl1-5* under ammonium conditions, virtually completely suppressing the
400 difference in growth (Figure S6a). Expression of *ALMT1* was upregulated in Col shoots
401 and roots under 10 mM ammonium compared with under 10 mM nitrate, and this
402 ammonium induction was significantly suppressed in *chl1-5* shoots and roots (Figure
403 S6b). Importantly, the magnitude of ammonium induction and suppression by *NRT1.1*
404 deficiency of *ALMT1* was much larger in shoots than in roots (Figure S6b). This
405 corresponds to the observation that the impact of *NRT1.1* deficiency on shoot growth
406 intensified compared to root growth (Figure 1k). These suggest that NRT1.1
407 exacerbates acidic stress in the presence of ammonium, mainly in shoots. Interestingly,
408 an acidic rhizosphere induces *NRT1.1* expression in a STOP1 transcription
409 factor-dependent way, which enhances symport of proton and nitrate through NRT1.1
410 and adjusts rhizosphere pH to a more suitable range (Ye et al. 2021). Furthermore,
411 NRT1.1 and SLAH3 collaborate to drive a nitrate cycle across the plasma membrane,
412 reducing acidification of the rhizosphere (Xiao et al. 2022). It is uncertain how NRT1.1
413 affects intra- and extracellular pH under nitrate-free ammonium conditions.

414 Our transcriptome analysis highlighted the extracellular space as an early site of
415 NRT1.1 action (Figure 3c, d, and S3a, b, S4b, c). A study by Podgórska et al. (2017) in
416 Arabidopsis plants demonstrated that ammonium toxicity is associated with smaller

417 mesophyll cells characterized by a more rigid cell wall structure, containing increased
418 phenolic compounds and boron ions. In our study, the GO terms “plant-type cell wall
419 loosening” and “plant-type cell wall modification” were enriched in the genes
420 upregulated by *NRT1.1* deficiency (Figure 3c and S4b). These terms originated from
421 genes encoding proteins involved in cell wall loosening and cell expansion, such as
422 *AT1G69530* (*EXPA1*), *AT1G74670* (*GASA6*), *AT2G20750* (*EXPB1*), *AT2G40610*
423 (*EXPA8*), *AT3G29030* (*EXPA5*), and *AT4G28250* (*EXPB3*). This suggests that NRT1.1
424 might influence ammonium tolerance via alterations in cell wall modification processes.
425 We discovered that genes for aliphatic GSL biosynthesis and their positive
426 regulator genes, *MYB28* and *MYB29*, were induced by *NRT1.1* deficiency (Figure 4a,
427 S2b, Table S2, 4). Coleto et al. (2021) reported that ammonium toxicity was
428 exacerbated in the *myb28myb29* mutant but not in the *myc234* mutant. Given that both
429 mutants are almost devoid of aliphatic GSL, the ammonium hypersensitivity of
430 *myb28myb29* is not linked with a lack of aliphatic GSL. The authors provided evidence
431 that MYB28 and MYB29 maintain intracellular iron homeostasis under ammonium
432 conditions, thereby attenuating ammonium toxicity. It remains to be seen whether the
433 absence of NRT1.1 enhances ammonium tolerance via upregulation of *MYB28* and
434 *MYB29*. Meanwhile, our transcriptome data suggested that NRT1.1 enhances ethylene
435 signaling under ammonium conditions. Plants emit ethylene as a phytohormone in
436 response to various stresses, including ammonium toxicity (Britto and Kronzucker
437 2002). Inhibition of ethylene signaling by gene knockout and chemical treatment
438 alleviates ammonium toxicity (Jian et al. 2018, Li et al. 2019). These findings suggest

439 that NRT1.1 reduces ammonium tolerance through ethylene signaling. Although there is
440 little overlap among aliphatic GSL biosynthesis genes and ACC- and low
441 pH-responsive genes (Tables S5, 6, 10), it would be worthwhile to scrutinize these
442 associations.
443

444 **Acknowledgments**
445 We are grateful for Dr. Carine Alcon and Montpellier RIO Imaging on technical support
446 with confocal microscopy and for Ms. Mako Sakai on technical support with expression
447 analysis and on manuscript review. We would like to thank Dr. Yi-Fang Tsay
448 (Academia Sinica) for giving the Arabidopsis seeds. We would also like to thank Enago
449 (www.enago.jp) for the English language review.
450

451 **Disclosure statement**
452 The authors report there are no competing interests to declare.
453

454 **Funding**
455 This study was supported by the Grants-in-Aid from the Ministry of Education, Culture,
456 Sports, Science and Technology, Japan (No. 17K15237, 20K05771, 23K04978 to TH),
457 by the Inamori Foundation (to TH), by the Agropolis Foundation (No. 1502-405 to TH),
458 and by the Nagase Science and Technology Foundation (to TH).
459
460

461 **References**

462 Bouguyon, E., F. Brun, D. Meynard, M. Kubeš, M. Pervent, S. Leran, B. Lacombe et al.
463 2015. “Multiple mechanisms of nitrate sensing by Arabidopsis nitrate transceptor
464 NRT1.1.” Nature Plants 1: 15015. doi:10.1038/nplants.2015.15.

465

466 Bouguyon, E., F. Perrine-Walker, M. Pervent, J. Rochette, C. Cuesta, E. Benkova, A.
467 Martinière, L. Bach, G. Krouk, A. Gojon, and P. Nacry. 2016. "Nitrate controls root
468 development through posttranscriptional regulation of the NRT1.1/NPF6.3
469 transporter/sensor." Plant Physiology 172: 1237-1248. doi:10.1104/pp.16.01047.

470

471 Britto, D. T., and H. J. Kronzucker. 2002. "NH_4^+ toxicity in higher plants: a critical
472 review." Journal of Plant Physiology 159(6): 567-584. doi:10.1078/0176-1617-0774.

473

474 Coleto, I., I. Bejarano, A. J. Marín-Peña, J. Medina, C. Rioja, M. Burow, and D. Marino.
475 2021. "*Arabidopsis thaliana* transcription factors *MYB28* and *MYB29* shape ammonium
476 stress responses by regulating Fe homeostasis." New Phytologist 229(2): 1021-1035.
477 doi:10.1111/nph.16918.

478

479 Goda, H., E. Sasaki, K. Akiyama, A. Maruyama-Nakashita, K. Nakabayashi, W. Li, M.
480 Ogawa, Y. Yamauchi, J. Preston, K. Aoki et al. "The AtGenExpress hormone and
481 chemical treatment data set: experimental design, data evaluation, model data analysis

482 and data access." The Plant Journal 55(3): 526-542.
483 https://doi.org/10.1111/j.1365-313X.2008.03510.x.
484
485 Hachiya, T., Y. Mizokami, K. Mizokami, D. Tholen, C. K. Watanabe, and K. Noguchi.
486 2011. "Evidence for a nitrate-independent function of the nitrate sensor NRT1.1 in
487 *Arabidopsis thaliana*." Journal of Plant Research 124: 425-430.
488 doi:10.1007/s10265-010-0385-7.
489
490 Hachiya, T., J. Inaba, M. Wakazaki, M. Sato, K. Toyooka, A. Miyagi, M.
491 Kawai-Yamada, D. Sugiura, T. Nakagawa, T. Kiba, A. Gojon, and H. Sakakibara. 2021.
492 "Excessive ammonium assimilation by plastidic glutamine synthetase causes
493 ammonium toxicity in *Arabidopsis thaliana*." Nature Communications 12(1): 4944.
494 doi:10.1038/s41467-021-25238-7.
495
496 Harun, S., M. R. Abdullah-Zawawi, H. H. Goh, and Z. A. Mohamed-Hussein. 2020. "A
497 comprehensive gene inventory for glucosinolate biosynthetic pathway in *Arabidopsis*
498 *thaliana*." Journal of agricultural and food chemistry 68(28): 7281-7297.
499 doi:10.1021/acs.jafc.0c01916.
500
501 Hieno, A., H. A. Naznin, K. Inaba-Hasegawa, T. Yokogawa, N. Hayami, M. Nomoto, Y.
502 Tada, T. Yokogawa, Mi. Higuchi-Takeuchi, K. Hanada, M. Matsui, Y. Ikeda, Y. Hojo, T.
503 Hirayama, K. Kusunoki, H. Koyama, N. Mitsuda, and Y. Y. Yamamoto. 2019.

504 "Transcriptome analysis and identification of a transcriptional regulatory network in the
505 response to H_2O_2." Plant Physiology 180(3): 1629-1646. doi:10.1104/pp.18.01426.
506
507 Ho, C. H., S. H. Lin, H. C. Hu, and Y. F. Tsay. 2009. “CHL1 functions as a nitrate
508 sensor in plants.” Cell 138 (6): 1184-1194. doi:10.1016/j.cell.2009.07.004.
509
510 Hooper, C. M., I. R. Castleden, S. K. Tanz, N. Aryamanesh, and A. H. Millar. 2017.
511 "SUBA4: the interactive data analysis centre for Arabidopsis subcellular protein
512 locations." Nucleic Acids Research 45(D1): D1064-D1074. doi:10.1093/nar/gkw1041.
513
514 Ito, T., R. Motohashi, T. Kuromori, S. Mizukado, T. Sakurai, H. Kanahara, M. Seki, and
515 K. Shinozaki. 2002. "A new resource of locally transposed *Dissociation* elements for
516 screening gene-knockout lines in silico on the Arabidopsis genome." Plant Physiology
517 129 (4): 1695-1699. doi:10.1104/pp.002774.
518
519 Jian, S., Q. Liao, H. Song, Q. Liu, J. E. Lepo, C. Guan, J. Zhang, A. M. Ismail, and Z.
520 Zhang. 2018. "NRT1.1-related NH_4^+ toxicity is associated with a disturbed balance
521 between NH4+ uptake and assimilation." Plant Physiology 178(4): 1473-1488.
522 doi:10.1104/pp.18.00410.
523
524 Krouk, G., B. Lacombe, A. Bielach, F. Perrine-Walker, K. Malinska, E. Mounier, K.
525 Hoyerova, P. Tillard, S. Leon, K. Ljung, E. Zazimalova, E. Benkova, P. Nacry, and A.

526 Gojon. 2010. "Nitrate-regulated auxin transport by NRT1.1 defines a mechanism for
527 nutrient sensing in plants." Developmental Cell 18(6): 927-937.
528 doi:10.1016/j.devcel.2010.05.008.
529
530 Krouk, G., C. Carré, C. Fizames, A. Gojon, S. Ruffel, and B. Lacombe. 2015.
531 "GeneCloud reveals semantic enrichment in lists of gene descriptions." Molecular Plant
532 8 (6): 971-973. doi: 10.1016/j.molp.2015.02.005.
533
534 Kuromori, T., T. Hirayama, Y. Kiyosue, H. Takabe, S. Mizukado, T. Sakurai, K.
535 Akiyama, A. Kamiya, T. Ito, and K. Shinozaki. 2004. "A collection of 11800
536 single-copy Ds transposon insertion lines in Arabidopsis." The Plant Journal 37(6):
537 897-905. doi: 10.1111/j.1365.313x.2004.02009.x.
538
539 Lager, I. D. A., O. L. A. Andréasson, T. L. Dunbar, E. Andreasson, M. A. Escobar, and A.
540 G. Rasmusson. 2010. "Changes in external pH rapidly alter plant gene expression and
541 modulate auxin and elicitor responses." Plant, Cell & Environment 33(9): 1513-1528.
542 doi:10.1111/j.1365-3040.2010.02161.x.
543
544 Li, G., L. Zhang, M. Wang, D. Di, H. J. Kronzucker, and W. Shi. 2019. "The
545 Arabidopsis *AMOT1/EIN3* gene plays an important role in the amelioration of
546 ammonium toxicity." Journal of Experimental Botany 70(4): 1375-1388.
547 doi:/10.1093/jxb/ery457.

Liu, K. H., Y. Niu, M. Konishi, Y. Wu, H. Du, H. S. Chung, L. Li, M. Boudsocq, M. McCormack, S. Maekawa, T. Ishida, C. Zhang, K. Shokat, S. Yanagisawa, and J. Sheen. 2017. “Discovery of nitrate-CPK-NLP signalling in central nutrient-growth networks.” Nature 545: 311-316. doi:10.1038/nature22077.

Liu, X. X., Y. X. Zhu, X. Z. Fang, J. Y. Ye, W. X. Du, Q. Y. Zhu, X. Y. Lin, and C. W. Jin. 2020. "Ammonium aggravates salt stress in plants by entrapping them in a chloride over-accumulation state in an NRT1.1-dependent manner." Science of The Total Environment 746: 141244. doi:10.1016/j.scitotenv.2020.141244.

Liu, K. H., M. Liu, Z. Lin, Z. F. Wang, B. Chen, C. Liu, A. Guo, M. Konishi, S. Yanagisawa, G. Wanger, and J. Sheen. (2022). "NIN-like protein 7 transcription factor is a plant nitrate sensor." Science, 377(6613), 1419-1425. doi: 10.1126/science.add1104.

Mounier, E., M. Pervent, K. Ljung, A. Gojon, and P. Nacry. 2014. "Auxin-mediated nitrate signalling by NRT1.1 participates in the adaptive response of *Arabidopsis* root architecture to the spatial heterogeneity of nitrate availability." Plant, Cell and Environment 37(1): 162-174. doi:10.1111/pce.12143.

Okamoto, Y., T. Suzuki, D. Sugiura, T. Kiba, H. Sakakibara, and T. Hachiya. 2019. "Shoot nitrate underlies a perception of nitrogen satiety to trigger local and systemic

570 signaling cascades in *Arabidopsis thaliana*." Soil Science and Plant Nutrition 65 (1):
571 56-64. doi:10.1080/00380768.2018.1537643.
572
573 Patterson, K., T. Cakmak, A. Cooper, I. D. A. Lager, A. G. Rasmusson, and M. A.
574 Escobar. 2010. "Distinct signalling pathways and transcriptome response signatures
575 differentiate ammonium- and nitrate-supplied plants." Plant, cell & environment 33(9):
576 1486-1501. doi:10.1111/j.1365-3040.2010.02158.x.
577
578 Podgorska, A., M. Ostaszewska, P. Gardeström, A. G. Rasmusson, and B. Szal. 2015.
579 "In comparison with nitrate nutrition, ammonium nutrition increases growth of the
580 frostbite1 Arabidopsis mutant." Plant, Cell and Environment 38(1): 224-237.
581 doi:10.1111/pce.12404.
582
583 Podgórska, A., M. Burian, K. Gieczewska, M. Ostaszewska-Bugajska, J. Zebrowski, D.
584 Solecka, and B. Szal. 2017. "Altered cell wall plasticity can restrict plant growth under
585 ammonium nutrition." Frontiers in Plant Science 8: 1344. doi:10.3389/fpls.2017.01344.
586
587 Remans, T., P. Nacry, M. Pervent, S. Filleur, E. Diatloff, E. Mounier, P. Tillard, B. G.
588 Forde, and A. Gojon. 2006. "The Arabidopsis NRT1.1 transporter participates in the
589 signaling pathway triggering root colonization of nitrate-rich patches." Proceedings of
590 the National Academy of Sciences of the United States of America 103 (50):
591 19206-19211. doi:10.1073/pnas.0605275103.

592

593 Riveras, E., J. M. Alvarez, E. A. Vidal, C. Oses, A. Vega, and R. A. Gutiérrez. 2015.
594 "The calcium ion is a second messenger in the nitrate signaling pathway of
595 Arabidopsis." Plant Physiology 169 (2): 1397-1404. doi:10.1104/pp.15.00961.

596

597 Shen, X., Z. Wang, X. Song, J. Xu, C. Jiang, Y. Zhao, C. Ma, and H. Zhang. 2014.
598 "Transcriptomic profiling revealed an important role of cell wall remodeling and
599 ethylene signaling pathway during salt acclimation in Arabidopsis." Plant Molecular
600 Biology 86: 303-317. doi:10.1007/s11103-014-0230-9.

601

602 Sun, J., & N. Zheng. 2015. "Molecular mechanism underlying the plant NRT1.1
603 dual-affinity nitrate transporter." Frontiers in Physiology 6 386. doi:
604 10.3389/fphys.2015.00386.

605

606 Tsay, Y. F., J. I. Schroeder, K. A. Feldmann, and N. M. Crawford. 1993a. "The herbicide
607 sensitivity gene *CHL1* of Arabidopsis encodes a nitrate-inducible nitrate transporter."
608 Cell 72 (5): 705-713. doi:10.1016/0092-8674(93)90399-B.

609

610 Tsay, Y. F., M. J. Frank, T. Page, C. Dean, and N. M. Crawford. 1993b. "Identification
611 of a mobile endogenous transposon in *Arabidopsis thaliana*." Science 260 (5106):
612 342-344. doi: 10.1126/science.838580.

613

614 Vidal, E. A., V. Araus, C. Lu, G. Parry, P. J. Green, G. M. Coruzzi, and R. A. Gutiérrez.
615 2010. "Nitrate-responsive miR393/AFB3 regulatory module controls root system
616 architecture in *Arabidopsis thaliana*." Proceedings of the National Academy of Sciences.
617 107 (9): 4477-4482. doi:10.1073/pnas.0909571107.
618
619 Walch-Liu, P., and B. G. Forde. 2008. "Nitrate signalling mediated by the NRT1.1
620 nitrate transporter antagonises L-glutamate-induced changes in root architecture." The
621 Plant Journal 54(5): 820-828. doi:10.1111/j.1365-313X.2008.03443.x.
622
623 Wang, R., R. Tischner, R. A. Gutiérrez, M. Hoffman, X. Xing, M. Chen, G. Coruzzi,
624 and N. M. Crawford. 2004. “Genomic analysis of the nitrate response using a nitrate
625 reductase-null mutant of Arabidopsis.” Plant Physiology 136 (1): 2512-2522.
626 doi:10.1104/pp.104.044610.
627
628 Wang, W., B. Hu, A. Li, and C. Chu. 2020. "NRT1.1s in plants: functions beyond nitrate
629 transport." Journal of Experimental Botany 71(15): 4373-4379. doi:10.1093/jxb/erz554.
630
631 Xiao, C., D. Sun, B. Liu, X. Fang, P. Li, Y. Jiang, M. He, J. Li, S. Luan, and He, K.
632 2022. "Nitrate transporter NRT1.1 and anion channel SLAH3 form a functional unit to
633 regulate nitrate-dependent alleviation of ammonium toxicity." Journal of Integrative
634 Plant Biology 64(4): 942-957. doi:10.1111/jipb.13239.
635

Ye, J. Y., W. H. Tian, M. Zhou, Q. Y. Zhu, W. X. Du, Y. X. Zhu, X. X. Liu, X. Y. Lin, S. J. Zheng, and C. W. Jin. 2021. "STOP1 activates NRT1.1-mediated nitrate uptake to create a favorable rhizospheric pH for plant adaptation to acidity." The Plant Cell 33(12): 3658-3674. doi:10.1093/plcell/koab226.

Zhang, X., Y. Cui, M. Yu, B. Su, W. Gong, F. E. Balu¡ka, G. Komis, J. Šamaj, X. Shan, J. Lin. 2019. Phosphorylation-mediated dynamics of nitrate transceptor NRT1.1 regulate auxin flux and nitrate signaling in lateral root growth. Plant Physiology 181 (2): 480-498. doi:10.1104/pp.19.00346.

Zhou, Y., B. Zhou, L. Pache, M. Chang, A. H. Khodabakhshi, O. Tanaseichuk, C. Benner, and S. K. Chanda. 2019. "Metascape provides a biologist-oriented resource for the analysis of systems-level datasets." Nature Communications 10(1): 1523. doi:10.1038/s41467-019-09234-6.

658 **Figure legends**

659 **Figure 1.** Plasma membrane-targeted NRT1.1 reduces ammonium tolerance almost
660 regardless of its phosphorylating status. (a, b) Fresh weights (FWs) of shoots from
661 11-day-old Col, *chl1-5*, *nrt1.1*, L*er*, *chl1-6*, Nossen, and *pst16286* plants grown under
662 10 mM ammonium (a) or 10 mM nitrate (b) conditions (Mean ± SD; n = 5-10). (c, d)
663 Shoot FWs in Col and NRT1.1-mCherry (eNRT1.1) lines under the control of the
664 β-estradiol-inducible promoter in the *chl1-5* background (Mean ± SD; n = 15). In one
665 dish, five seedlings of each line grown under the 10 mM nitrate condition for 5 days
666 were transferred to the 10 mM ammonium (c) or 10 mM nitrate (d) condition in the
667 absence (ethanol as a mock) or presence of 1 μM β-estradiol and further grown for 6
668 days. (e, f) Shoot FWs (e) and a representative photograph (f) from 11-day-old Col,
669 *chl1-5*, *chl1-9* (*P492L*), *T101D*, and *T101A* plants grown under 10 mM ammonium
670 conditions (Mean ± SD; n = 5). The scale bar represents 5 mm. Twelve shoots from one
671 plate were regarded as a single biological replicate. (g) The chlorophyll (*a* + *b*)
672 concentrations of shoots from 5-day-old Col, *chl1-5*, *chl1-9*, *T101D*, and *T101A*
673 seedlings grown under 10 mM ammonium (Mean ± SD; n = 3). Thirty-seven shoots
674 from one plate were regarded as a single biological replicate. (h, i) FWs of shoots from
675 11-day-old Col and *cipk23-4* plants grown under 10 mM ammonium (h) or 10 mM
676 nitrate (i) conditions (Mean ± SD; n = 5-10). (j) FWs of 3-day-old Col and *chl1-5*
677 seedlings grown under 10 mM ammonium (Mean ± SD; n = 4). (k) FWs of shoots and
678 roots from 5-, 8-, or 11-day-old Col and *chl1-5* grown under 10 mM ammonium (Mean
679 ± SD; n = 5). (l) Representative photographs of 3-day-old Col and *chl1-5* seedlings

680 grown under 10 mM ammonium and representative photographs of the adaxial side of
681 cotyledons from 5-day-old Col and *chl1-5* seedlings grown under 10 mM ammonium.
682 The scale bars represent 1 mm (3-day) and 500 μm (5-day). (a, b, h–k) Six shoots or
683 roots from one plate were regarded as a single biological replicate. In one dish, six seeds
684 of each line of wild-type and mutant were placed and grown. *$P < 0.05$; **$P < 0.01$;
685 ***$P < 0.001$ (unpaired two-tailed Welch's *t*-test). NS denotes not significant. Different
686 lowercase letters indicate significant differences evaluated by the Tukey–Kramer
687 multiple comparison test conducted at a significance level of $P < 0.05$.
688
689 **Figure 2.** NRT1.1 is expressed in various tissues under ammonium conditions. (a)
690 Relative transcript levels of *NRT1.1* in 3-day-old Col whole seedlings grown under 10
691 mM ammonium or 10 mM nitrate conditions (Mean ± SD; n = 3). 45 seedlings from
692 one plate were regarded as a single biological replicate. (b) Relative transcript levels of
693 *NRT1.1* in shoots and roots from 5-, 8-, or 11-day-old Col grown under 10 mM
694 ammonium or 10 mM nitrate conditions (Mean ± SD; n = 3). 12 shoots and 12 roots
695 from one plate were regarded as a single biological replicate. (c–j) Signals of
696 NRT1.1-GFPloop from pavement cells of cotyledons from 3-day-old plants (c),
697 epidermal cells of hypocotyl from 3-day-old plants (d), mesophyll protoplasts from
698 12-day-old plants (e), root cap and epidermal cells near primary root tips from
699 5-day-old plants (f, g), primary root tip from 5-day-old plants (h), and pavement cells of
700 cotyledons from 8-day-old plants (i: horizontal central section of the cell, j: horizontal
701 section below the cell surface layer) grown under 10 mM ammonium condition except

702 for mesophyll protoplasts from 12-day-old plants (e). Mesophyll protoplasts were
703 prepared from the plants which were grown under 10 mM nitrate for 9 days, then
704 transferred to 10 mM ammonium, and further grown for 3 days. The scale bars
705 represent 10 μm (c, e–j) and 30 μm (d). The purple signals represent autofluorescence
706 (e) and PI fluorescence (f). The images were processed by Image J version 1.53c. Figure
707 2h was generated by the maximum intensity projection.
708
709 **Figure 3.** Genome-wide transcriptional responses caused by *NRT1.1* deficiency. (a)
710 Venn diagram showing the number of genes upregulated and downregulated in the 3-
711 and 5-day-old *NRT1.1*-deficient mutants (*chl1-5*, *nrt1.1*) compared with Col grown
712 under 10 mM ammonium. The transcripts whose expression was at least 1.5-fold
713 (3-day) or 2-fold (5-day) higher or at most 1/1.5 (3-day) or 1/2 lower (5-day) in both
714 mutants relative to that in Col were counted. The gene lists are shown in Supplementary
715 Tables S2, 3. (b) Outputs derived from GeneCloud analysis of genes upregulated and
716 downregulated in the 3-day-old *NRT1.1*-deficient mutants (*chl1-5*, *nrt1.1*) compared
717 with Col grown under 10 mM ammonium. The numbers next to the term denote the
718 number of genes containing the term and the fold enrichment. (c, d) Outputs derived
719 from Metascape analysis of genes upregulated (c) and downregulated (d) in the
720 3-day-old *NRT1.1*-deficient mutants (*chl1-5*, *nrt1.1*) compared with Col grown under 10
721 mM ammonium. Note that microarray analysis was conducted using 3-day-old (72 h)
722 and 5-day-old (120 h) whole seedlings of Col, *chl1-5*, and *nrt1.1*.
723

724 **Figure 4.** NRT1.1 primarily alters the expression of aliphatic glucosinolate biosynthesis
725 genes, ACC-responsive genes, and low pH-responsive genes under ammonium
726 conditions. (a–f) Comparisons of the expression of biosynthesis genes for aliphatic
727 glucosinolate (AGSL) and indole glucosinolate (IGSL) (a), genes upregulated and
728 downregulated by ACC application (b), genes upregulated and downregulated by NaCl
729 stress (c), genes upregulated and downregulated by H_2O_2 application (d), genes
730 upregulated and downregulated by IAA application (e), and genes upregulated and
731 downregulated by low pH treatment (f) between Col and *NRT1.1*-deficient mutants
732 (*chl1-5*, *nrt1.1*) grown under 10 mM ammonium. The samples harvested from two
733 independent experiments were subjected to microarray analysis. E1 and E2 denote 1st
734 experiment and 2nd experiment, respectively. One hundred thirty-five seedlings (3-day)
735 from three plates and 74 seedlings (5-day) from two plates were regarded as a single
736 biological replicate. Changes in gene expression levels between Col and *chl1-5* and Col
737 and *nrt1.1* were represented as logarithms to base 2 of ratios in signal intensities. *1-5*
738 and *1.1* denote *chl1-5* and *nrt1.1*, respectively. $^{*}P < 0.05$; $^{**}P < 0.01$; $^{***}P < 0.001$
739 (two-tailed ratio paired *t*-test).

Figure 1

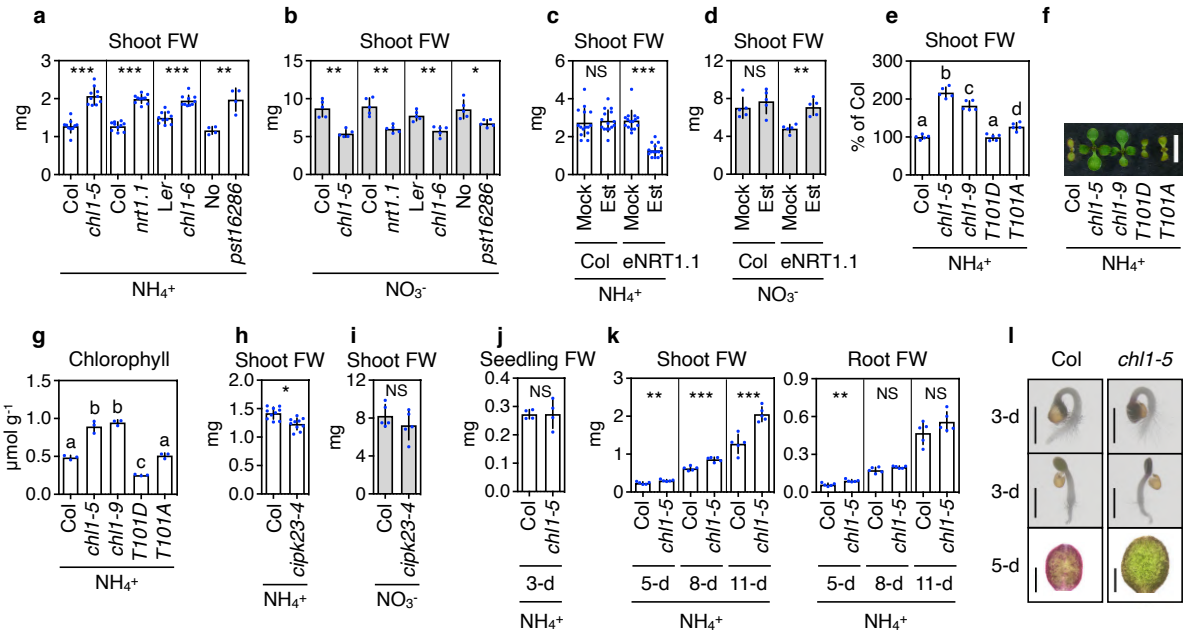
a
Shoot FW
mg
Col
chl1-5
nrt1.1
Ler
chl1-6
No
pst16286
NH4+
b
Shoot FW
NO3-
c
Shoot FW
NS
Mock
Est
Col
eNRT1.1
d
Shoot FW
e
Shoot FW
% of Col
chl1-9
T101D
T101A
f
g
Chlorophyll
µmol g-1
h
i
cipk23-4
j
Seedling FW
3-d
k
Root FW
5-d
8-d
11-d
l
Col
chl1-5

Figure 2

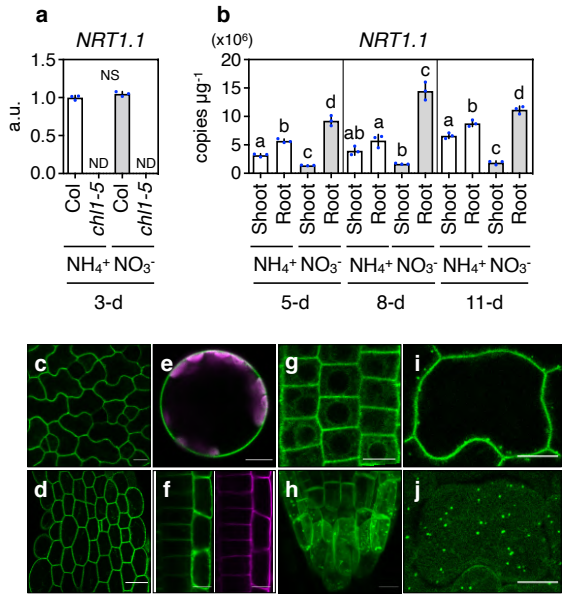
a
NRT1.1
a.u.
1.5
1.0
0.5
0.0
NS
ND
ND
Col
chl1-5
Col
chl1-5
NH4+ NO3-
3-d
b
(x10^6)
NRT1.1
copies µg-1
20
15
10
5
0
a
b
c
d
ab
a
b
c
a
b
c
d
Shoot
Root
Shoot
Root
Shoot
Root
Shoot
Root
Shoot
Root
Shoot
Root
NH4+ NO3-
NH4+ NO3-
NH4+ NO3-
5-d
8-d
11-d
c
e
g
i
d
f
h
j

Figure 3

a

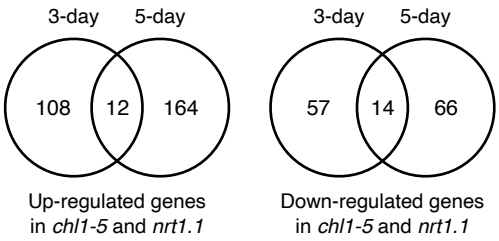

b

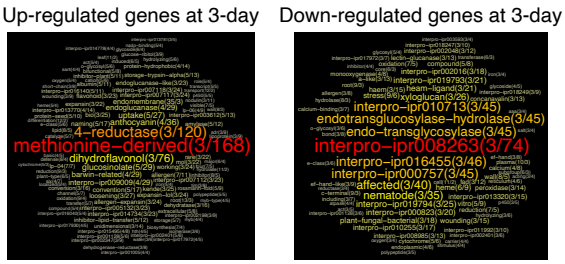

c

GO Biological Processes/KEGG Pathway/WikiPathways for Up-regulated genes at 3-day

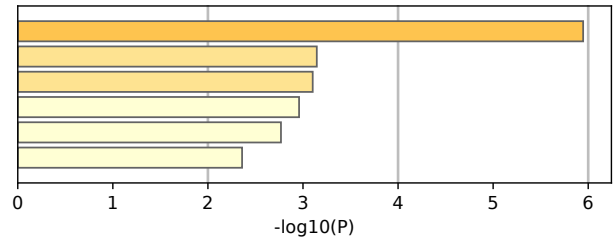

WP4597: Glucosinolate biosynthesis from methionine
GO:0009682: induced systemic resistance
GO:0009812: flavonoid metabolic process
GO:0009828: plant-type cell wall loosening
ath00910: Nitrogen metabolism - Arabidopsis thaliana (thale cress)
GO:0051049: regulation of transport

GO Cellular Components for Up-regulated genes at 3-day

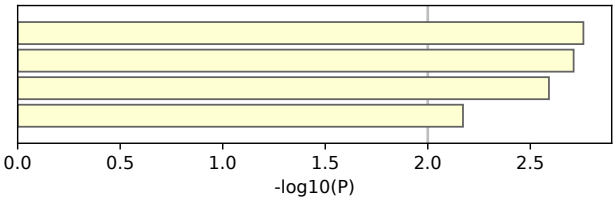

GO:0019867: outer membrane
GO:0009707: chloroplast outer membrane
GO:0099503: secretory vesicle
GO:0048046: apoplast

GO Molecular Functions for Up-regulated genes at 3-day

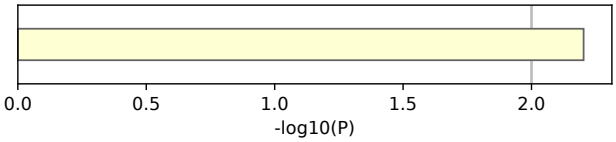

GO:0016836: hydro-lyase activity

d

GO Biological Processes/KEGG Pathway/WikiPathways for Down-regulated genes at 3-day

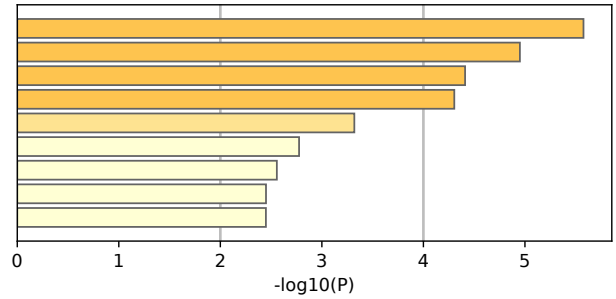

GO:0009651: response to salt stress
GO:0071456: cellular response to hypoxia
GO:0014070: response to organic cyclic compound
GO:0010200: response to chitin
GO:0010411: xyloglucan metabolic process
GO:0006979: response to oxidative stress
ath04146: Peroxisome - Arabidopsis thaliana (thale cress)
GO:0071369: cellular response to ethylene stimulus
GO:0009409: response to cold

GO Cellular Components for Down-regulated genes at 3-day

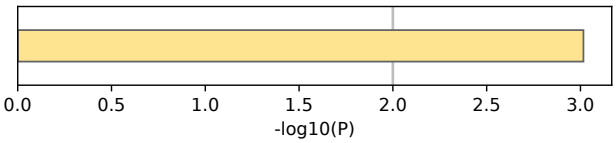

GO:0009505: plant-type cell wall

GO Molecular Functions for Down-regulated genes at 3-day

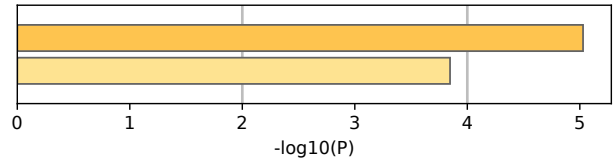

GO:0016209: antioxidant activity
GO:0016762: xyloglucan:xyloglucosyl transferase activity

Figure 4

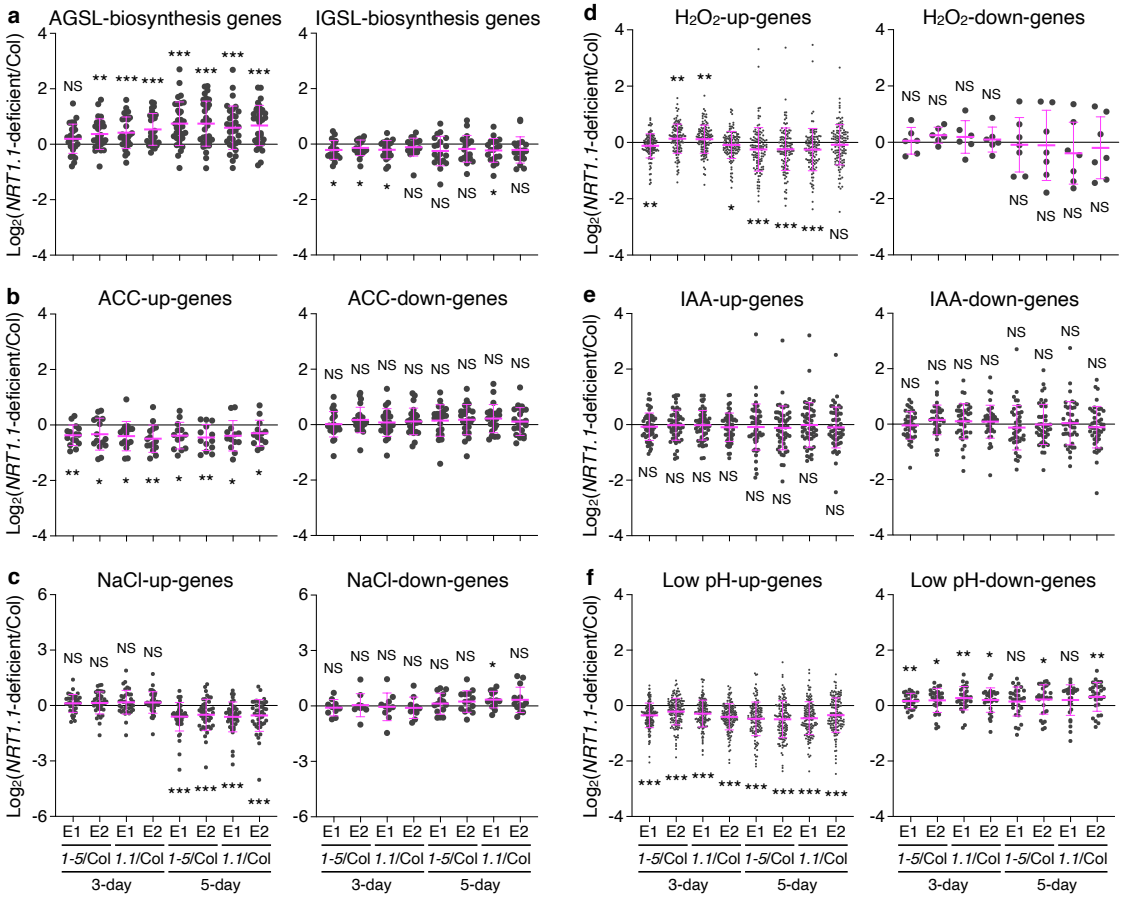
a
AGSL-biosynthesis genes
IGSL-biosynthesis genes
b
ACC-up-genes
ACC-down-genes
c
NaCl-up-genes
NaCl-down-genes
d
H2O2-up-genes
H2O2-down-genes
e
IAA-up-genes
IAA-down-genes
f
Low pH-up-genes
Low pH-down-genes
Log2(NRT1.1-deficient/Col)
E1 E2 E1 E2 E1 E2 E1 E2
1-5/Col 1.1/Col 1-5/Col 1.1/Col
3-day
5-day